

Biexciton states in semiconductor microcavities

T. Baars, G. Dasbach, M. Bayer, and A. Forchel

Technische Physik, Universität Würzburg, Am Hubland, 97074 Würzburg, Germany

(Received 21 January 2000; revised manuscript received 12 December 2000; published 3 April 2001)

A planar semiconductor microcavity in the strong coupling regime has been studied by spectrally resolved degenerate four wave mixing using femtosecond laser pulses. At high excitation densities, new spectral features observed besides the cavity polaritons can be uniquely identified as of biexcitonic origin. We investigate the dispersion of these features with cavity detuning. The observations are compared to several model descriptions for the interaction of the biexciton with the cavity light field.

DOI: 10.1103/PhysRevB.63.165311

PACS number(s): 71.36.+c, 42.50.Md, 78.47.+p

Since the pioneering work of Weisbuch *et al.*¹ semiconductor microcavities have attracted great interest. In particular, the optical properties in the so-called strong coupling regime have been investigated extensively in the last few years.^{2,3} In this regime the dipole coupling strength is large compared to the homogeneous linewidth of the exciton and photon. In this case excitons and cavity photons form a pair of new, coupled eigenmodes, so-called cavity polaritons, that exhibit a pronounced anticrossing behavior.^{1,4} Recently, the nonlinear optical properties of these quasiparticles have become a very active field of theoretical and experimental research.⁵⁻⁹

Less attention has been paid to nonlinear effects related to the formation of biexcitons. Previously, these biexcitonic nonlinearities have been invoked in the interpretation of coherent effects in microcavities.¹⁰ More recently it has been demonstrated that biexcitonic effects enhance the Rabi splitting between the two polariton branches.¹¹ These findings are in agreement with theoretical calculations.¹² Recently, a clear observation of biexcitons in microcavities has been reported.¹³ However, no systematic results for the dispersion of the biexcitonic mode as function of the energy separation between the exciton and the optical mode had been given there. The formation of biexcitons and bipolaritons in microcavity structures has been discussed theoretically.^{14,15} It was concluded that bipolaritons are not sufficiently stable in the limiting cases where the bare biexciton binding energy is either significantly larger or smaller than the Rabi splitting and only biexcitons formed by dark excitons are of physical relevance. These predictions are in good agreement with experimental pump-and-probe studies on a microcavity, where the Rabi splitting is considerably larger than the biexciton binding energy.¹⁶

In this paper we address the point at issue where the biexciton binding energy ($V_{biX} \approx 2.2$ meV) is comparable to the exciton-photon coupling ($\hbar\Omega = 3.8$ meV). The results have been obtained in spectrally resolved four-wave-mixing (FWM) studies. As FWM allows the separation of excitonic and biexcitonic contributions due to their different polarization selection rules, this technique is well suited to study biexcitonic effects in semiconductor quantum structures. The observation of additional modes in the FWM spectrum and a characteristic beat frequency of the signal can be clearly attributed to the coherent superposition of two-particle states. The experimental results are compared to several models for

the interaction of the two exciton complex with the confined light field in the cavity based either on weak or strong interaction. The observations can best be described in a strong coupling model. As origin for the strong interaction we envisage a strong reabsorption of photons, arising from the radiative decay of an electron-hole pair in a biexciton, by the background of excitons. The coupling strength thus depends on the number of electron-hole pairs in the cavity.

We have investigated a microcavity sample containing a single 7 nm wide $\text{In}_x\text{Ga}_{1-x}\text{As}$ ($x=0.14$) quantum well (QW) at the antinode of a λ GaAs cavity. The top (bottom) mirror consists of 21 (23) pairs of distributed Bragg reflectors with a reflectivity of 99.5%. The cavity length and thus the detuning $\Delta = E_c - E_x$ between the cavity mode E_c and the heavy-hole exciton mode E_x could be varied by changing the position of the laser spot on the sample. At resonance ($\Delta = 0$) the transmission spectrum shows a Rabi splitting of 3.8 meV and a linewidth of 1.0 meV and 1.2 meV for the upper (UPB) and lower (LPB) polariton branch, respectively. From the literature we estimate a biexciton binding energy of $V_{biX} \approx 2.2$ meV for the QW embedded in the cavity.^{17,18}

Spectrally resolved, time-integrated FWM experiments were performed in the two-pulse self-diffracting transmission geometry¹⁹ using a femtosecond mode-locked Ti:sapphire laser. In this configuration two short pulses having wave vectors \mathbf{k}_1 and \mathbf{k}_2 are focused onto the same spot on the sample. The two pulse trains hit the sample symmetrically under an angle of 3° relative to the cavity normal. For such small angles effects due to the angular dispersion of the polariton modes can be neglected. The FWM signal emitted in the direction $2\mathbf{k}_2 - \mathbf{k}_1$ is spectrally resolved by a monochromator and detected by a liquid-nitrogen-cooled charge-coupled device camera as a function of photon energy E and of the delay τ between the two pulses. The laser pulses had a duration of ~ 80 fs corresponding to a spectral width of ~ 30 meV [full width at half maximum (FWHM)]. The spectral resolution of the system is ~ 0.1 meV and the experiments were performed at $T = 2$ K. The intensity of the exciting pulses corresponds to a polariton density in the microcavity of $\sim 10^{11} \text{ cm}^{-2}$ as estimated from reflection measurements. In this range the FWM signal is to a good approximation proportional to the third power of the laser intensity.

Figure 1(a) shows a contour plot of the FWM signal close to the cavity resonance ($\Delta = 0.8$ meV) as a function of de-

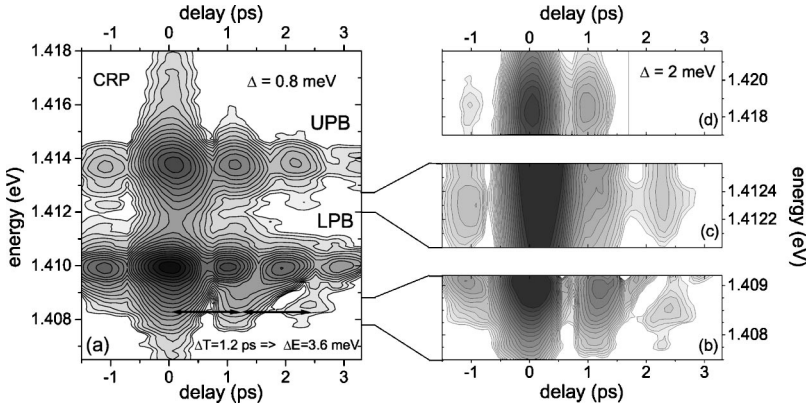


FIG. 1. Logarithmic contour plots of the FWM signal for cross-polarized excitation and a cavity detuning of $\Delta = 0.8$ meV [(a)–(c)]. The arrows in (a) mark the beat period of the FWM signal at the spectral feature at $E \approx 1.4085$ eV. (b) and (c) are closeups of (a) as indicated. In (b) the LPB signal has been subtracted for clarity. (d) shows the FWM signal above the UPB for a detuning $\Delta = 2.0$ meV.

tection energy and delay between the pulses. The exciting pulses were cross-linearly polarized (CL), i.e., they had linear but orthogonal polarizations. The dominant features are the signals from the UPB at ≈ 1.414 eV and from the LPB at ≈ 1.410 eV. The oscillations superimposed on the decay of the signal are due to quantum beats caused by the coherent superposition of the two states.²⁰ The beat period of about 1 ps corresponds to the splitting of the two modes in the spectral domain of ≈ 4 meV. Below the LPB an additional spectral feature can be seen at an energy slightly below 1.409 eV.²¹ This signal oscillates with a frequency different from the polariton beat frequency, as indicated by the arrows. The additional mode is shown more clearly on a small energy scale in Fig. 1(b), where we have subtracted the LPB signal so that the feature is resolved as a separate peak. Its beat period of $\Delta T \approx 1.15$ ps corresponds to an energy separation of $\Delta E \approx 3.6$ meV. A weak spectral line corresponding to this energy separation is tentatively identified below the UPB at $E \approx 1.4123$ eV. As can be seen from the enlarged plot in Fig. 1(c). This line displays the same beat frequency as the low-energy feature. The occurrence of an extra mode between the polariton branches agrees with the theoretical calculations of Sieh *et al.*¹²

Additionally, we also observe a FWM signal on the high-energy side approximately 4 meV above the UPB [see Fig. 1(d)]. However, this signal is only visible for larger positive detuning ($\Delta \approx 2$ meV). The appearance of the spectral feature may be explained by effects due to nondegenerate

FWM, since both polariton branches are excited simultaneously by the laser pulses. Nondegenerate FWM leads to a mode with energy $2E_{UPB} - E_{LPB}$. The calculated detuning dependence of this non-degenerate FWM signal is in good agreement with the experimental data (see Fig. 3).

To investigate the origin of the additional peaks in the FWM signal we varied the polarization of the exciting pulses. Figure 2 shows the FWM spectrum taken at a delay of 1.5 ps for collinear and cocircular excitation. The low-energy peak disappears for excitation with cocircularly polarized beams. In this configuration biexcitonic FWM signals are suppressed, since the biexciton as a spin singlet state can be excited only in the presence of both σ_+ and σ_- polarized light. We therefore attribute this additional emission to biex-

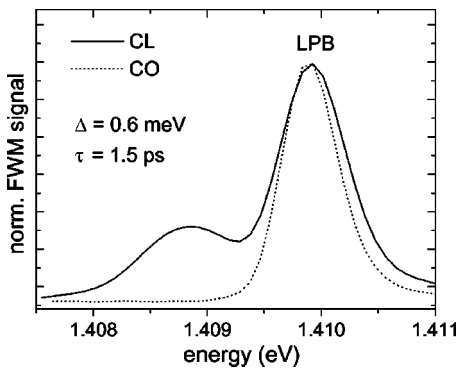


FIG. 2. FWM spectra for cross-linearly polarized (CL, full line) and co-circularly polarized (CO, dotted line) excitation at a delay of $\tau = 1.5$ ps and a cavity detuning of $\Delta = 0.6$ meV.

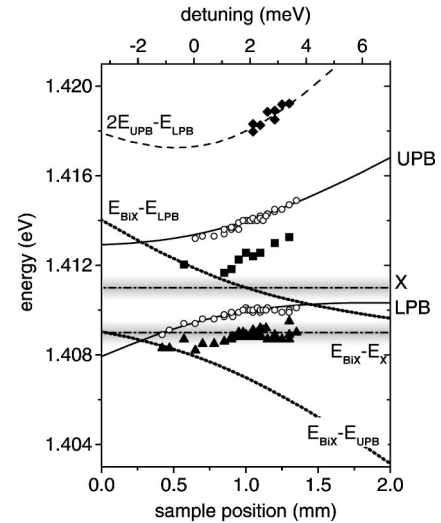


FIG. 3. Energies of the modes observed in the FWM spectra versus cavity detuning (top scale) and sample position (bottom scale). The symbols correspond to the experimental data, where the open symbols describe the lower and upper polariton branches and the full symbols represent transitions to hybridized two-particle states. The solid lines represent the fitted dispersion of the upper and lower polariton branch. The dotted lines display the transition energies obtained from biexciton-polariton transitions. The upper shaded region marks the energy range of uncoupled excitons. The lower shaded range indicates the exciton-biexciton transitions. The dashed curve represents the dispersion of the non-degenerate FWM signal.

citonic contributions and the beating of this signal to the coherent superposition with an additional two-particle state. The different oscillation periods of this feature as compared to the polaritons facilitate the spectral resolution of the biexciton: At $\tau=1.5$ ps the contribution of the LPB to the FWM signal is minimal, while the contribution of the mode on its low-energy side reaches a maximum.

The spectral positions of the various modes observed in the FWM signal are shown in Fig. 3 as a function of the detuning Δ . For the upper and lower polariton branch (open symbols) we observe the well-known anticrossing behavior: At positive detuning the LPB becomes excitonlike with a constant energy, while the UPB becomes photonic with strong dispersion. At negative detuning the two branches exchange their character. The mode splitting at zero detuning is in good agreement with the Rabi splitting measured in low-density transmission experiments. This indicates that the experiments are performed well within the strong coupling regime. The biexcitonic mode below the LPB (triangles in Fig. 3) shows only weak dispersion and the energy splitting from the LPB seems to decrease for negative detunings. The mode below the UPB (squares) which is also involved in the beating shifts strongly to lower energies as the detuning decreases.

We will now present several models by which the additional spectral features in the FWM spectra could be explained. In these approaches the extra modes are described by transitions from two- onto one-particle states.

(1) An obvious model treats transitions from the biexciton state onto the polariton branches: Any binding of two excitons, even if very weak, would involve wave numbers that extend significantly beyond the region in which strong coupling occurs, which for the studied cavity is $k_0 \approx 10^6 \text{ m}^{-1}$.¹⁶ If the spatial extension of the biexciton wave function is estimated to be comparable to the exciton Bohr radius, one can estimate that in reciprocal space wave numbers at least one order of magnitude larger than k_0 are involved in the binding. Therefore the interaction of the biexciton with the cavity light field should be weak. The energies of these transitions as function of the cavity detuning are diagrammed by the dotted lines in Fig. 3. Obviously these modes are not in agreement with the experimental findings. Note that the dashed line in Fig. 3 gives the energy of the nondegenerate FWM signal calculated from the polariton energies.

(2) A somewhat better approximation to the data can be achieved by relating the observed two-particle states to transitions from excitons localized in QW potential fluctuations to biexcitons. In contrast to free excitons, such excitons are pinned in real space and consequently their wave functions are spread out in momentum space. This leads to a weak interaction between the cavity mode and the localized states, due to the small overlap of their wave functions. These states are distributed over a certain energy range corresponding to the inhomogeneous broadening of the exciton. The upper shaded region in Fig. 3 indicates the spectral range of the localized excitonic states. The lower shaded region represents the possible transition energies between the uncoupled biexciton and the localized excitons assuming an average biexciton binding energy of 2.2 meV, which is typical for

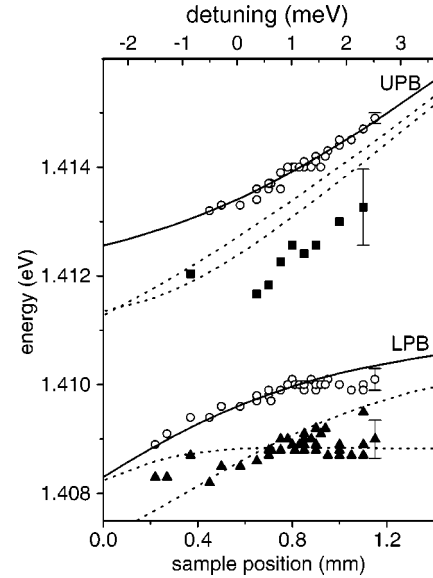


FIG. 4. Experimental data as discussed in the captions of Fig. 3. The dotted lines are calculated results obtained by the bipolaritonic approach.

GaAs-based quantum wells. This mode matches well the spectral feature observed on the low-energy side of the LPB.

Only for negative detunings we observe a small discrepancy between the calculated energy and the experimental data. This might be explained by filtering effects of the cavity due to the spectral variation of the cavity transmission: For negative detunings the spectral position of the LPB shifts to lower energies and therefore the transmission maximum of the cavity is shifted to the red. This shift can also effect the position of the spectral feature on the low-energy side of the LPB and lead to the observed redshift. However, the model cannot explain the spectral feature between the two polariton branches. Although its shift with detuning might also be related to a filter effect, its energy difference to the biexciton state is too large to be related to a coherent superposition of the biexciton with the state of two unbound excitons.

(3) We present here an additional approach, which allows for describing the observations in a satisfactory way. In this model we assume that the transition from a one- to a two-particle state shows a strong interaction with the confined light field. A vivid picture for this interaction might be given in the following way. Let us assume a rather high density of electron-hole pairs, as in the present experiments. One of the two electron-hole pairs forming a biexciton might then decay radiatively. Due to the elevated carrier density the resulting photon forms again a biexciton when being reabsorbed. The strength of this interaction process naturally depends on the number of electron-hole pairs available. The coupled exciton-photon system can be described in the following way.

For the one-particle excitations we apply the standard coupled oscillator model leading to a 2×2 matrix Hamiltonian.²

$$\mathcal{H}_1 = \hbar \begin{pmatrix} \omega_X^{\pm}(\Delta) & \Omega/2 \\ \Omega/2 & \omega_C^{\pm}(\Delta) \end{pmatrix}.$$

Here $\hbar\Omega$ is the vacuum Rabi splitting, which is a measure of the strength of the light-matter interaction, which occurs between excitations of the same spin only. $\hbar\omega_C(\Delta)$ and $\hbar\omega_X(\Delta)$ are the eigenenergies of the cavity mode and the excitonic mode. The hybridized exciton-photon states are given by the eigenvalues of the matrix. This description for polaritons has been demonstrated to be an excellent approximation for particle densities well below the Mott density for the transition to an electron-hole plasma.^{22,23} In microcavities the transition to the high-density regime is characterized by breaking of the strong coupling between excitons and photons, leading to a decrease in the polaritonic normal mode splitting. The present experiments obviously were performed in a density regime where the polaritonic coupling remains unbroken, giving justification for this treatment. The experimental data for the polariton branches (open symbols in Fig. 3) have been fitted by the solutions of \mathcal{H}_1 . From the

fit (solid line in Fig. 3) we obtain the uncoupled exciton and photon energies that will be used as input parameters for model presented in the following.

The two-particle excitations are described in a coupled four-level model, in which excitations of opposite and identical spin orientation have to be distinguished. We are interested here only in bound complexes; therefore two-particle states with the same circular polarization will not be discussed here. In the anticircular case, the uncoupled eigenstates are the two-photon, two states consisting of a photon and an exciton states of opposite polarizations and the two-exciton state, which is the biexciton. Their energies form the diagonal elements of the matrix representation. To obtain the coupled ‘‘bipolaritonic’’ states we have to take into account the interaction between those two-particle states.

Here we consider only the interaction processes in which one of the two excitations is converted, while we set the interaction matrix elements for the two-particle conversions to zero. These processes should have a rather small probability. This leads to the following effective 4×4 matrix Hamiltonian:

$$\mathcal{H}_2^{+-} = \hbar \begin{pmatrix} \omega_X^- + \omega_X^+ - V_{BiX}/\hbar & \Omega'/2 & \Omega'/2 & 0 \\ \Omega'/2 & \omega_C^+ + \omega_X^- & 0 & \Omega'/2 \\ \Omega'/2 & 0 & \omega_X^+ + \omega_C^- & \Omega'/2 \\ 0 & \Omega'/2 & \Omega'/2 & \omega_C^+ + \omega_C^- \end{pmatrix}.$$

Here $\hbar\Omega'$ is the interaction matrix element. From the expression for the square of the vacuum Rabi splitting $\hbar\Omega$, which is proportional to the number of elementary cells in the quantum well, we expect that $\hbar\Omega'$ is proportional to the square root of the exciton density. By diagonalizing \mathcal{H}_2^{+-} the energies of the coupled two-particle complexes are obtained, from which we determine the energies of the transitions onto the polaritons. For these calculations the parameters obtained above together with a biexciton binding energy $V_{biX} = 2.2$ meV are taken as input parameters. Ω' is determined from a fit to the experimental data.

The calculated energy differences as function of the cavity detuning are shown by the dotted lines in Fig. 4. From the eight possible transitions only four have energies in the range of interest. For $\hbar\Omega' = 3.5$ meV we obtain good agreement between experiment and model for the present excitation density. A sensitive test for this model would be the dependence of the interaction strength Ω' on the excitation power. However, in the present experiments such a test was not possible. If we reduce the excitation power the signal from the biexcitonic contributions becomes too weak to be resolved as function of the detuning. If we increase the exci-

tation, on the other hand, the strong coupling regime breaks down. It remains a future task to perform this test, for example, by studying samples with a larger exciton binding energy and Rabi-splitting, respectively.

In conclusion we have identified two-particle states in an $\text{In}_x\text{Ga}_{1-x}\text{As}/\text{GaAs}$ microcavity that exhibit biexcitonic signatures. Several models are presented for describing the dependence of these features on the cavity detuning. An interpretation in terms of biexciton-polariton transitions does not match with the experimental findings. Also, a biexciton-localized exciton model does not give satisfactory agreement. The additional modes can be understood, however, in the framework of a bipolariton formalism. A more detailed theoretical description for biexcitons in microcavities similar to those established for quantum wells²⁴ remains to be developed in the future but is beyond the scope of the present paper.

This work has been supported financially by the Deutsche Forschungsgemeinschaft and the State of Bavaria. We gratefully acknowledge enlightening discussions with P. Hawrylak. We thank F. Schäfer and J. P. Reithmaier for the growth of the microcavity sample.

- ¹C. Weisbuch, M. Nishioka, A. Ishikawa, and Y. Arakawa, *Phys. Rev. Lett.* **69**, 3314 (1992).
- ²For a recent review see, e.g., M.S. Skolnick, T.A. Fisher, and D.M. Whittaker, *Semicond. Sci. Technol.* **13**, 645 (1998).
- ³See, e.g., *Confined Electrons and Photons, New Physics and Applications*, Vol. 340 of NATO Advanced Study Institute Series B: Physics, edited by E. Burstein and C. Weisbuch (Plenum, New York, 1995).
- ⁴R. Houdré, C. Weisbuch, R.P. Stanley, U. Oesterle, P. Pellandini, and M. Illegems, *Phys. Rev. Lett.* **73**, 2043 (1994).
- ⁵P.G. Savvidis, J.J. Baumberg, R.M. Stevenson, M.S. Skolnick, D.M. Whittaker, and J.S. Roberts, *Phys. Rev. Lett.* **84**, 1547 (2000).
- ⁶R. Houdré, C. Weisbuch, R.P. Stanley, U. Oesterle, and M. Illegems, *Phys. Rev. Lett.* **85**, 2793 (2000).
- ⁷G. Dasbach, T. Baars, M. Bayer, A. Larionov, and A. Forchel, *Phys. Rev. B* **62**, 13 076 (2000).
- ⁸Le Si Dang *et al.*, *Phys. Rev. Lett.* **81**, 3920 (1999).
- ⁹P. Senellart and J. Bloch, *Phys. Rev. Lett.* **82**, 1233 (1999).
- ¹⁰M. Kuwata-Gonokami *et al.*, *Phys. Rev. Lett.* **79**, 1341 (1997); M. Shirane *et al.*, *Phys. Rev. B* **58**, 7978 (1998).
- ¹¹X. Fan, H. Wang, H.Q. Hou, and B.E. Hammons, *Phys. Rev. B* **57**, R9451 (1998).
- ¹²C. Sieh, T. Meier, A. Knorr, F. Jahnke, P. Thomas, and S.W. Koch, *Eur. Phys. J. B* **11**, 407 (1999).
- ¹³U. Neukirch, S.R. Bolton, N.A. Fromer, L.J. Sham, and D.S. Chemla, *Phys. Rev. Lett.* **84**, 2215 (2000).
- ¹⁴V.M. Agranovich, G.C. La Rocca, and F. Bassani, *Phys. Status Solidi A* **164**, 39 (1997).
- ¹⁵G.C. La Rocca, F. Bassani, and V.M. Agranovich, *J. Opt. Soc. Am. B* **15**, 652 (1998).
- ¹⁶P. Borri, W. Langbein, U. Woggon, J.R. Jensen, and J.M. Hvam, *Phys. Rev. B* **62**, R7763 (2000).
- ¹⁷T. Baars, W. Braun, M. Bayer, and A. Forchel, *Phys. Rev. B* **58**, R1750 (1998).
- ¹⁸P. Borri, W. Langbein, J.M. Hvam, and F. Martelli, *Phys. Rev. B* **60**, 4505 (1999).
- ¹⁹See, e.g., J. Shah, *Ultrafast Spectroscopy of Semiconductors and Semiconductor Nanostructures* (Springer-Verlag, Berlin, 1996).
- ²⁰H. Wang, J. Shah, T.C. Damen, W.Y. Jan, J.E. Cunningham, M. Hong, and J.P. Mannaerts, *Phys. Rev. B* **51**, 14 713 (1995).
- ²¹Note that this low-energy feature cannot be related to charged excitons. First, the feature disappears for weak excitation powers. Second, the polarization selection rules for the FWM signal from trions [H.P. Wagner, H.-P. Tranitz, and R. Schuster, *Phys. Rev. B* **60**, 15 542 (1999)] are different from those demonstrated in Fig. 2.
- ²²E. Hanamura and H. Haug, *Phys. Rep., Phys. Lett. C* **33**, 209 (1977).
- ²³F. Tassone and Y. Yamamoto, *Phys. Rev. B* **59**, 10 830 (1999).
- ²⁴See, e.g., A.L. Ivanov, H. Haug, and L.V. Keldysh, *Phys. Rep.* **296**, 237 (1998).